UC Irvine
UC Irvine Electronic Theses and Dissertations

Title

Stabilization, Shrinkage and Future Applications of Bulk Nanobubbles

Permalink

https://escholarship.org/uc/item/4vb806tp

Author

Satpute, Pratik

Publication Date

2019

Peer reviewed|Thesis/dissertation

UNIVERSITY OF CALIFORNIA,
IRVINE

Stabilization, Shrinkage and Future Applications of Bulk Nanobubbles

THESIS

submitted in partial satisfaction of the requirements
for the degree of

MASTER OF SCIENCE

in Materials Science & Engineering

by

Pratik Ashutosh Satpute

Thesis Committee:
Professor James C. Earthman, Chair
Professor Ruqian Wu
Associate Professor Daniel Mumm

2019

DEDICATION

To

my parents, teachers and friends

in recognition of their worth

for their belief

Whatever the work a man performs,
The most effective aid to its completion,
The most prolific source of its success,
Is energy, not despondency

Vālmiki
The Ramayana

and patience

Every great dream begins with a dreamer. Always remember, you have within you the strength, the patience, and the passion to reach for the stars to change the world.

Harriet Tubman

TABLE OF CONTENTS

Page

LIST OF FIGURES

ACKNOWLEDGMENTS

I would like to express the deepest appreciation to my committee chair, Professor James Earthman, who has the sheer patience and the endurance associated with the quintessential great researcher: he continually and convincingly conveyed a spirit of adventurous inquiry in regard to research, and an excitement in regard to teaching. Without his guidance and persistent help this dissertation would not have been possible.

I would like to thank my committee members, Professor Ruqian Wu and Professor Daniel Mumm, whose work demonstrated to me that an attention to detail, progressing from and keeping the fundamentals strong is crucial to the building of an idea.

In addition, a thank you to Professor Jacob Brouwer of the National Fuel Cell Research Centre, who introduced me to fuel cells, and whose belief in fuel cells and capacity for novelty had lasting effect.

Lastly, I would like to thank my parents and friends, whose support and care over the past two years has enabled me to maintain my focus and keep to the path I chose.

ABSTRACT OF THE THESIS

Stabilization, Shrinkage and Future Application of Bulk Nanobubbles

By

Pratik Ashutosh Satpute

Master of Science in Materials Science & Engineering

University of California, Irvine, 2019

Professor James C. Earthman, Chair

We describe a theoretical framework for predicting bulk nanobubble size of any given combination of a gas and water, based upon the force balance at the gas/liquid interface. We show how this balance can develop between the internal pressure, external pressure and surface tension, and the electrostatic repulsion of hydroxide ions adhered to the surface of the nanobubble that gives rise to their relatively high negative zeta potential. We also analyse the adsorption of hydroxide ions at the surface of the nanobubble and the dependence of nanobubble formation on pH and the required initial size of a bubble that leads to the formation of a stable nanobubble. Further analysis is carried out on the velocity of the bulk nanobubble due to Brownian motion, and its effects on the rates of diffusion of the gas into the water, as well analysis on the interaction between hydroxide ions and oxygen molecules to infer the inhibition of their diffusion. Future applications and methodologies for applications, based on the equations proposed are also discussed.

INTRODUCTION

The dictionary definition of the prefix 'nano' indicates that the object or dimension it describes is in the range of 10^{-9} of the dimensions it is described by, and it is as such that nanobubbles have become popular, under a misnomer. Many prefer the name ultrafine bubbles, since the size range of nanobubbles begins at one micron, and usually goes down much further to only as few as 10 nanometers in diameter. Since their discovery as the remains of collapsing microbubbles and of their persistence after formation, attempts have been consistently to understand the mechanics of their dissolution and stability, to enable the design of systems that use them to our advantage.

The first field to experience benefits due to micro- and nanobubbles was agriculture, and the use of nanobubble water was well-documented by several studies since the year 2000, showing increased growth and quality of root vegetables grown in hydroponic systems, as well as the cultivation of tomatoes in soil. Further benefits were also demonstrated with pisciculture, showing increased sizes of the fish cultured in nanobubble water, due to an increase in the dissolved oxygen content. Similar benefits were also demonstrated in the case of shrimp breeding, due to the same phenomenon. However, all of these systems were simply a case of using the equipment for generating microbubbles without much control, and to permit them to dissolve into the water without regard for optimization. Indeed, without any parameters to measure the rate of dissolution and the generation and stability of the generated bubbles, it is not possible to optimize such a system. Thus, ongoing research has focused on the generation, stability and control of these bubbles for diverse application in the fields of drug delivery, water treatment, energy storage, and various others.

The second technological application of microbubbles was for the treatment of water based on the release of hydroxide ions from collapsing microbubbles, which shed light on one particular area, which was a promising candidate for explaining the stability of the nanobubble. The focus of stability was discovered by measurement of the zeta-potential of the first microbubbles of about 2 microns in diameter, which was found to be about -35 mV, and is still thought to be the cloud of ions that exists around a nanobubble. This suggested a role of the surrounding cloud of ions in their stability, in particular their ability to inhibit diffusion of the gas into the fluid, which has given rise to several theories regarding the mechanism of the ions' stabilizing influence. Several approaches have also been made for specific cases such as surface nanobubbles and electrochemically generated bubbles, which involve several scenarios of diffusion and shrinkage. The work that is outlined here will summarize and look for theoretical evidence and alternatives to the presented theories, as well as present a new argument for the mechanism of stability of bulk nanobubbles, which seeks to incorporate and explain as many of the observed behaviors of nanobubble systems as possible. A further analysis of possible future applications is also presented.

CHAPTER 1

1.1 The Problem of Stability

The stability of nanobubbles, especially bulk nanobubbles, is described essentially by the Young-Laplace equation, which is

$$p_{int} = p_{ext} + \frac{2\gamma}{r}$$

Where p_{int} is the internal pressure, p_{ext} is the external pressure, γ is the surface tension, and r is the radius of the nanobubble. The scientific consensus is that the internal pressure of the bubble is not high enough to balance both the external pressure, which is a combination of the pressure exerted by the water column above the bubble as well as atmospheric pressure, and the pressure exerted by the surface tension, which seeks to reduce the surface area of the nanobubble. Both of these contribute to the pressure differential across the nanobubble surface that essentially forces the bubble to collapse, with the gas leaving the bubble by diffusing into the bulk solvent. Given the small amounts of gas within the bubbles, this should, in theory, take a very small amount of time to diffuse and disperse, causing the nanobubble to shrink to nothing almost instantly. However, the lifetime of nanobubbles has bene measured in the hours, if not days, which shows that the process of diffusion should be inhibited in some way, and that the pressure is, in effect, balanced or very nearly so.

However, if this is indeed the case, there must be a mechanism and a third component in the system which causes the inhibition of the diffusion, and which, by extension, exerts a pressure that opposes the surface tension and the external pressure, along with the internal pressure. The third component is suspected to be the hydroxide ion, which is always present

in aqueous solutions, and which is detected around collapsing microbubbles, and has already been applied to wastewater treatment. This ion tends to aggregate around the nanobubble surface, and is suspected to be present in the form of a cloud of ions around the bubble, attracted to the surface by an as yet unconfirmed force, but widely thought to be physical bonds of the nature of van der Waal's force, and plays a part in the inhibition of gas diffusion out of the bubble.

The exact mechanism, distribution of the ions, the extent to which they inhibit the diffusion, and other concerns regarding their roles in the mechanism of stabilization is not yet determined, but several theories have been proposed as to their role, and more also exist which do not take into account their role, or do not require them to play any role in the process at all. The role of the ions is suspected to be due to the repulsion of the ions toward each other, which in some way opposes the external pressure and the surface tension, but this is yet to be confirmed. Thus, while there are several approaches to the question, as of recent efforts it still remains unresolved.

1.2 Objective of Present Study

The objective of the present study is to offer a theoretical explanation for the stability of bulk nanobubbles, and the effect of environmental conditions on phenomenon, as well as to use the same theory to explain some of the properties of nanobubbles that have been observed and reported.

CHAPTER 2

2.1 Literature Survey

2.1.1 Stability of Bulk Nanobubbles

Several theoretical approaches have been proposed, many of which are highly specific to the circumstances for which the study was conducted, and none thus far have proposed an overarching theory as to the formation and evolution of bulk nanobubbles. As far back as 1997 Ljunggren and co-workers [1] proposed theoretical explanations for colloid-sized gas bubbles based on diffusion of the gas into the liquid, which could now be considered nanobubbles. Seddon et. al. [2] also contributed to the emerging idea around the same time, but there have been few contributions to understanding their stable presence since then. Explanations for specific cases of phenomena such as surface nanobubbles, nanobubbles generated electrochemically, and so forth have been offered so far. Early on, the Young-Laplace equation was used to describe nanobubble stability [3], but the internal pressures required are far higher than would be possible at ambient temperature for the amount of gas that is contained within the bubble. Attard and co-workers [4] analysed the thermodynamic stability of bulk nanobubbles, but it was found that the radius of nanobubbles could not be accurately predicted from thermodynamic considerations, nor was an expression offered for the rate of decrease in nanobubble size. Brenner and Lohse [5] presented a model for predicting the radius of surface bubbles based on the dynamic equilibrium between diffusion into and out of nanobubbles situated at a surface. Further work in specific cases by Weijs and Lohse [6] suggested the use of increased length scales to counter the problem of high internal pressures due to the relatively high surface tension of a bubble in that size range. Sverdrup

and colleagues [7] offered explanations as to the rates of decrease in size based on diffusion in all directions possible through the gas-water interface at the nanobubble surface. In their models they consider the possibility of diffusion both into and out of the nanobubble, with a sufficiently high mass transfer coefficient. Their models consist of a combination of Henry's Law and Taylor series expansion. The equations are plotted, taking time as a function of radius and show coherence with previous models given by Ljunggren. However, no comparisons with experimental data are provided.

The size of the nanobubble depends on the balance of the surface forces which are holding it together. The Young-Laplace equation seems inadequate to completely describe the phenomenon as it requires extremely high internal pressures of the gas to balance the surface tension that causes the nanobubble to shrink, as summarized by Attard and co-workers [4]. However, the interface through which the diffusion occurs has thus far been considered to have constant properties of being composed only of water molecules and gas molecules.

Yasui and colleagues [8] also detail several theories that attempt to explain bulk nanobubble stability, based on the armoured bubble model, a particle crevice theory, a skin theory, the dynamic equilibrium model and electrostatic repulsion. Among these theories, it appears that electrostatic repulsion has the most experimental support. Studies of interfaces between water and practically all surfaces such as glass are negatively charged, assumed to be due to the accumulation of hydroxide ions physisorbed to the monolayer as reported by Zangi and Engberts [9]. Thus, it is reasonable to suppose that the water-gas interface is also negatively charged due to similar congregation of hydroxide ions at the bubble surface.

Furthermore, studies conducted by Takahashi and others [10, 11] have shown that nanobubbles are indeed negatively charged, with oxygen nanobubbles having a zeta potential about -35 mV. Thus, it is evident that hydroxide ions physisorbed onto the surface of the nanobubble play a role in the interactions between the molecules present there. Jin et. al. [12] proposed a model for bulk nanobubble stability involving the electrostatic repulsion, terming the pressure due to the electrostatic force as Maxwell pressure. One rationale involving the surface charge density of a bulk nanobubble has been proposed by Ahmed and colleagues [13] that involves electrostatic repulsion balancing the surface tension. In the following, we consider a theory of electrostatic repulsion and what it requires of the conditions imposed for nanobubbles to have the long-term stability that has been observed experimentally [3].

2.1.2 Applications of Nanobubbles

Several applications have been discovered, such as for wastewater treatment, fish farming, shrimp breeding, and hydroponics. These are further substantiated by Agarwal and co-workers [14], for such specific issues as the disinfection of infected surfaces, the degradation of organic compounds, and the disinfection of the water itself. The effects of increased yield of fish due to higher dissolved oxygen content are summarised by Endo et al. [15, 16]. The usage of hydrogen nanobubbles in gasoline to improve the calorific yield is also reported by Oha et al. [17]. Other projected uses include the use of nanobubbles as contrast agents for the ultrasound imaging of tumours, as reported by Cai and co-workers [18], as well as reduction and removal of deposits of calcium oxalate, which is similar to the composition of kidney stones in rat kidneys, as presented by Hirose et al [19]. Another application of the

nanobubble's ability to permit salts to crystallize is the design of self-cleaning membranes for desalination of water, which use nanobubbles as electrically conductive spacers and pass current through them to force the salts to crystallize on the nanobubble surface, which will permit easy removal of the accumulated salts. This was demonstrated and presented by Abida et al [20].

CHAPTER 3

3.1 Pressure, Force Balance and Stabilization

The pressure balance of the nanobubble is considered to be given by the Young-Laplace equation, which, as explained above, equates the internal pressure, external pressure and the surface tension. The first of the four forces that we consider in the Young-Laplace equation is internal pressure. It is proportional to the surface area of the nanobubble, and is assigned a positive sign since it acts to increase surface area. The second is the external pressure, given by the hydrostatic pressure acting on the surface of the bubble, which also decreases the surface area and is negative. The third is the surface tension, which acts along the surface area at the molecular level. The surface tension acts to decrease the surface area, hence the radius and size, and can also be assigned the negative sign.

However, a fourth force which is thought to be integral to the stability is the electrostatic repulsion between hydroxide ions adsorbed to the surface of the nanobubble, or, possibly in the cloud surrounding the surface. This repulsion seeks to reduce the contact between the ions on the surface of the bubbles, which also acts to increase the distance between the ions, thus increasing the surface area, and therefore results in a positive pressure.

The nature of the interaction between ions can be characterized by the expression for Coulombic repulsion. Since one hydroxide ion is of the order of 1 nanometre in diameter, and most nanobubbles are two orders of magnitude greater in size, we can ignore the curvature of the distance between them and take it to be linear. The repulsion should, in theory, affect all neighbouring hydroxide ions, but is assumed to be insignificant beyond the nearest

neighbours. We also assume the spatial arrangement of these ions over the surface to be close-packed in nature, since the repulsion is equal in all directions, and they would ideally assume a close-packed formation. This arrangement of ions is shown schematically below, in Fig. 1a, and as shown in Fig 1b) it is assumed, due to close-packing, that they assume the formation of a rhomboidal unit cell, of side and diagonal length denoted by x, which will be referred to subsequently as the inter-ionic distance.
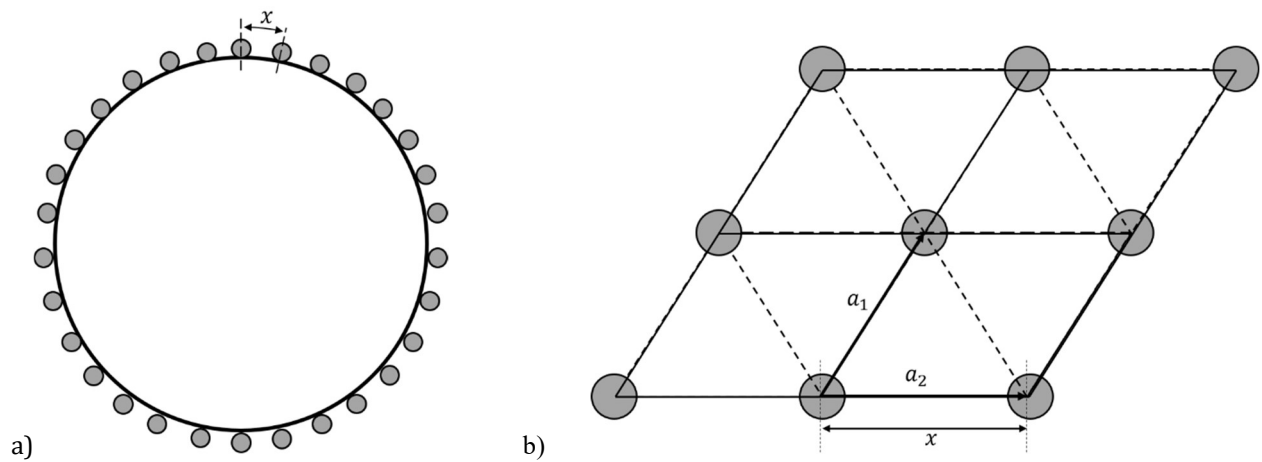

a)   b)

Figure 1: a) Schematic diagram of hydroxide ions adhered to the surface. Grey circles indicate the positions of the hydroxide ions. b) Close-packed arrangement of four unit cells of hydroxide ions over the surface of the nanobubble.

3.2 Derivation of the Force Balance

The pressures described by the Young-Laplace equation can be written down in representative form as,

$$p_{int} + p_{F_i} = p_{ext} + p_{st} \tag{1}$$

where p_{F_i} is the pressure due to the force of repulsion of negative ions adsorbed onto the bubble surface, and p_{st} the pressure due to the surface tension.

A force balance can be obtained by substituting the ideal gas law for the force due to the internal pressure, and inserting the expression for surface tension over a spherical area, which gives,

$$\left(\frac{nRT}{\frac{4\pi}{3}r^3} \times 4\pi r^2\right) + F_i = \left((p_{external}) \cdot 4\pi r^2\right) + 2\gamma\pi r \tag{2}$$

where n is the number of moles of gas present within the nanobubble, and F_i is the ionic repulsion force.

Replacing the external pressure with the hydrostatic and atmospheric pressure, results in,

$$\frac{3nRT}{r} + F_i = \left((\rho g h + P_0) \cdot 4\pi r^2\right) + 2\gamma\pi r \tag{3}$$

where ρ is the density of the fluid, g is the acceleration due to gravity, and h is the height in the fluid column where the bubble exists, and P_0 is the atmospheric pressure.

The ionic repulsion force depends on the surface concentration of ions, and assuming a close-packed arrangement, we assume a hexagonal arrangement as shown in Fig 1b). The repulsion is simply caused by the Coulomb force between the ions, given by

$$F_i = \frac{k_e\,q^2}{x^2} \tag{4}$$

where k_e is the Coulombic constant for the fluid, and q is the charge on each adjacent hydroxide ions.

For a close-packed arrangement of ions, taking the unit cell defined by the vectors a_1 and a_2 as show in Fig. 1b), the area of one unit cell is,

$$A = \frac{\sqrt{3}}{2}x^2 \tag{5}$$

Considering that the surface of the entire sphere can be made up of N number of small rhombohedra of hydroxide ions, Equation (7) gives,

$$A_{sphere} = 4\pi r^2 = \frac{N\sqrt{3}}{2}x^2 \tag{6}$$

The relation between N and the surface charge s is given by,

$$N = \frac{s}{q} = \frac{\sigma \cdot 4\pi r^2}{q} \tag{7}$$

Substituting expression (7) in (6),

$$x^2 = \frac{2q}{\sqrt{3}\sigma} \tag{8}$$

It follows then that substituting Equation (8) into Equation (4) results in

$$F_i = \frac{\sqrt{3}k_e\,\sigma q}{2}$$ (9)

Inserting Equations (9) and (7) in Equation (3), and multiplying by r, the force balance becomes,

$$(\rho gh + P_0)\,4\pi r^3 + \gamma.2\pi r^2 - \left(\frac{\sqrt{3}}{2}k_e q\sigma\right) \cdot r - 3nRT = 0$$ (10)

CHAPTER 4

4.1 Shrinkage and Contributing Factors

That the nanobubble shrinks due to outward diffusion of the gas contained within is, of course, undisputed, but the precise methods and the rate of diffusion are highly debated. Previous theoretical studies (cite Sverdrup) have always assumed a model with a higher mass transfer coefficient, or longer time scales for the process to account for the reduced rate and the high lifetime of the nanobubble. However, it is reasonable to suggest that the change in the rate of diffusion can be attributed to two things: the velocity due to the Brownian motion of the nanobubble, and the inhibition of the diffusion due to the adsorbed hydroxide ions on the surface. In this chapter, the possible effects of Brownian motion are examined for the effect on the rate of diffusion that they may possess.

4.2 Brownian Motion and its Effects on Shrinkage

Earlier studies have shown that nanobubbles can be formed by supersaturation, where the solubility limit of the gas, when surpassed will permit the gas to precipitate and form bulk nanobubbles as reported by Matsuki and co-workers (2014) (*12*). The shrinkage of nanobubbles has so far been thought to be governed by Fick's Laws, since it is a case of how fast the gas can dissolve into the surrounding fluid. Thus, according to the first law, it must be directly proportional to the outward gas flux, but the constant is still the diffusion constant D_0 for the diffusion of the gas into water. However, this only holds true where the surface area of the nanobubble remains constant. It is, however, possible, that the outward diffusion is a case of Fick's second law, since the surface area that is available to the gas to diffuse outward also changes according to size, and that this surface area determines the rate of shrinkage and thus the lifetime of the bulk nanobubble. It is then reasonable to suppose that the cause of the change of surface area available for diffusion is the change in the surface area occupied by hydroxide ions combined with the decreasing radius of the bulk nanobubble.

The rationale for the assumption that the hydroxide ions adhere to and are released the nanobubble surface is based on two observations, as mentioned before. Firstly, the observation that all interfaces formed by water are negatively charged, and we consider nanobubbles to be a special case of a gas-water interface which may be charged in the same way. Secondly, the zeta potentials measured for nanobubbles are all negative, indicating that a negative ion present in pure water is responsible for the negative charge, which by elimination is the hydroxide ion. Further observations also indicate higher negative

potentials for more electronegative gases, such as oxygen and nitrogen, than for other reported gases such as argon and xenon as reported by Ushikubo et. al. [11]. That nano- and microbubbles release hydroxide ions as they shrink is a well-known phenomenon [22].

The stabilization and the shrinkage can be considered to be related to the same phenomenon; thus, the ideal case can be taken to be a nanobubble that is newly formed with no hydroxide ions at the surface at the instant of its formation of an interface. Here, the hydroxide ions present in the water immediately surrounding the bubble, in the hydrodynamic layer, adhere almost instantaneously, the time taken for the adsorption to occur being too small in comparison to the overall timescale to be important. As a concentration gradient is then formed between the water layers at the nanobubble surface and the bulk fluid, more hydroxide ions begin diffusing from the bubble through this diffusion layer to the surface of the bubble. The thickness of this layer can be found by Prandtl's equation, where the fluid velocity is the velocity of the Brownian motion of the bubble as predicted by the Langevin equation, using the Ornstein-Uhlenbeck process. The same layer also acts a diffusion region for protons, which diffuse in from the bulk layer once they are depleted or their concentration changes, and must also be affected by the distance they must diffuse through to reach the nanobubble surface. These phenomena are further examined in the following sections.

4.3 Calculation of Velocity

This velocity, however, has a higher stochastic component than nanoparticles of a similar size, since the density of the nanobubble is much lower than nanoparticles of materials such as silver or silicon, but most of these are directed toward changing the direction of the motion of the nanobubble. The Langevin equation for the nanobubble can be solved, as is shown below.

The friction coefficient for the nanobubble in water is:

$$f = 6\pi\eta r \qquad (11)$$

Where η is the Stokes viscosity of water in pascal-seconds, and r is the radius of the nanobubble.

The characteristic relaxation time for the nanobubble is, however, different due to the gaseous nature of the contents, and it is given as:

$$\tau_b = \frac{m}{\gamma} \qquad (12)$$

Replacing the mass with the number of moles multiplied by molar mass, as obtained from the previous treatment, we get,

$$\tau_b = \frac{nM}{f} \qquad (13)$$

We expect the relaxation time to be far lower, on the order of 10^3 times lower than for a solid nanoparticle of comparable size, since the mass of the nanobubble is nearly a thousand times lower than a comparable nanoparticle of, for example, gold. Additionally, this relaxation time

also decreases, being directly proportional to the radius. The Langevin equation, using the Ornstein-Uhlenbeck process gives us the expression for velocity, as:

$$v(t) = V = e^{\frac{-t}{\tau_b}} v(0) + \frac{1}{m} \int e^{\frac{-(t-s)}{\tau_b}} dW(s) \qquad (14)$$

where $v(0)$ is the velocity at the time of formation, and s is the time elapsed between two collisions. We can take $v(0)$ to be zero, since at $t = 0$, the bubble has just formed and beginning to experience Brownian motion, which gives us the equation,

$$v(t) = V = \frac{1}{m} \int e^{\frac{-(t-s)}{\tau_b}} dW(s) \qquad (15)$$

4.4 Thickness of the Diffusion Layer

Considering this velocity as the relative velocity of the bulk fluid to the nanobubble, we can find the Reynolds number for the flow, and considering it to be laminar due to the extremely small scale, we can obtain an expression for the boundary layer thickness, which is also the thickness of the fluid layer which the protons and hydroxide ions from the bulk fluid must travel through to reach the nanobubble surface. Thus, the thickness, from the velocity obtained is, according to the Blasius solution,

$$\delta = 4.91\sqrt{\frac{vx}{v}} \tag{16}$$

where v is the kinematic viscosity, and x is equal to the largest circumference of the nanobubble,

$$x = 2\pi r \tag{17}$$

4.5 Times of Diffusion

At the same time, protons from the diffusion layer also reach the hydroxide ion-rich surface, but much more slowly, at a rate about five times slower than the hydroxide ions. Upon reaching the surface, they start eliminating the hydroxide ions into water molecules, which further increases the dilution of both ions, and encourages diffusion from the bulk layer to the interface, which is probably a monolayer. When the three processes, of hydroxide diffusion, proton diffusion, and hydroxide elimination by protons, are in steady state or in dynamic equilibrium, we have a fixed amount of area which is not covered by hydroxide ions, however temporarily and will allow the diffusion of gas into the water. Taking an average, we can define a percentage of surface area of the nanobubble, which will remain available for diffusion, which will be in proportion to the radius of the bubble. This can be done by taking the size of one hydroxide ion, then finding the capacity of a nanobubble's surface to adsorb hydroxide ions, correlating it with the number of ions being eliminated, and taking a ratio with the capacity which is a function of area, which is a function of radius.

The rate at which the adsorption of the hydroxide ion takes place would then depend on two separate phenomena: firstly, the repulsion by the hydroxide ions already physisorbed onto the surface, which would force the ion to move along the surface until it finds a location that is unoccupied, and secondly, the velocity of the hydroxide ion as it travels through the hydrodynamic layer of the nanobubble. The velocity can be found by calculating the surface charge on the nanobubble, and using it and the initial distance between a particular ion to find the potential that drives it to move. The potential for the hydroxide ion to move to the nanobubble surface decreases as the surface charge increases, and thus the rate will

eventually dwindle down to zero as the bubble achieves stability, and the potential will reach a constant value.

The rate for the elimination of the physisorbed hydroxide ions, on the other hand, will only increase the surface charge density increases, since the elimination is accomplished by positively charged protons attracted to a negatively charged surface. The same equations for ionic mobility can be used to calculate the velocity of travel for the protons, but there is no equation needed for the rate of adsorption, as they simply react with the adsorbed hydroxide ion to give two molecules of water. The balance between these two rates thus depends on the time at which the reactions are taking place, which will ultimately determine the area needed for the diffusion of the gas into the water.

To find the ion mobility, we first consider an ideal case where a newly-formed and shrinking bubble has no hydroxide ions physisorbed onto its surface, and is formed in pure water with a pH of 7. This gives us, assuming a perfectly uniform distribution of ions in the water, a concentration of 10^{-7} moles of hydroxide and protons each in the surrounding hydrodynamic layer. Thus, the amount of both available to be physisorbed can be found by simply taking a section of the hydrodynamic layer up to the distance from the surface where we wish to find the concentration and time needed to reach the surface for the ions present at that distance from the surface. We take the volume of this section and multiply by molarity and Avogadro's number to get the actual number of ions present, as shown below.

$$p = \frac{4\pi}{3}[(r+d)^3 - d^3](10^{-7}) \tag{18}$$

Where p is the number of ions, r is the radius of the nanobubble, d is the distance from the from the surface of the nanobubble, and the 10^{-7} is the concentration of hydroxide ions in pure water of pH 7. For a differential thickness d_t, where d_t is the thickness that hydroxide ions can traverse to adhere to the nanobubble in a negligible amount of time, the surface charge Q becomes,

$$Q = p_t.e \qquad (19)$$

Where e is the elementary charge, and p_t is the number of ions physisorbed from a water layer of thickness of d_t.

Assuming that these, the closest ions, are physisorbed instantly, and that once the ions which are close enough that their time required for adsorption is smaller than the average needed for all the ions reach the surface they will be similarly physisorbed, a potential is established which depends directly upon time. This potential is used to find the ion mobility and thus the velocity of the ions that will follow. Thus, firstly, the potential is:

$$V = \epsilon \frac{e^2 p_t}{h} \qquad (20)$$

Where h is the thickness of the hydrodynamic layer as found from the Prandtl equation above, and ϵ is the permittivity of pure water.

The drift velocity of the protons attracted to the surface can then be found,

$$v = Vu \qquad (21)$$

where v is the drift velocity and u is the mobility of a proton.

This can be used to find the number of hydroxide ions being eliminated from the surface of the nanobubble, and thus to find the number of hydroxide ions left after the elimination. This then can be used to give us a percentage of total surface area of the nanobubble that is available for diffusion. The rate of diffusion of the gas into the water from the bubble can then be determined by Fick's Second Law, and thus we also find the time needed for the entire amount of gas within the nanobubble to diffuse into the water, giving us a prediction for the lifetime of the bubble. The equation for the time needed for a proton to reach the surface of the nanobubble can then be written as:

$$t = \frac{\delta}{v} \tag{22}$$

where t is the time needed for an ion to travel through the boundary layer. Thus, when t equals the time needed for one hydroxide ion to be physisorbed, a balance is formed between elimination and adsorption. Now, the rate of change of the diffusion area is constant, and depends directly upon the amount of gas left. At this time, the shrinkage will still continue until the hydroxide ions have no unoccupied surface area between them, and their repulsion will contribute to the fullest possible extent to counter surface tension and the external pressure to stabilize the size of the nanobubble.

The number of ions physisorbed to the surface, as mentioned in the previous section, can be found by equating the rates of travel and physisorption of hydroxide ions to the surface to the rate of protons eliminating them, as given by the equation:

$$N_{ion} = \frac{[OH^-]}{t} - \frac{[H]^+}{t_p} \tag{23}$$

24

where t_p is the time needed for the hydroxide ion to similarly diffuse through the boundary layer and be physisorbed onto the surface. The concentrations of hydroxide ions and protons comes from the difference between the concentration of hydroxide ions and protons in the bulk fluid at a given pH, and their concentration at the inner edge of the boundary layer, which is assumed to be zero.

The lifetime of the bubble, in the scenario described in the equations above, will then be the summation of the longest time that one proton can travel to reach the surface for each radius, until the point of stability, adding on the time needed for the surface area for the outward diffusion to reach zero. This can be written as,

$$\sum_{i=1}^{n} t_i = \sum_{i=1}^{n} \frac{\delta_i}{v_i} + t_d \qquad (24)$$

where t_d is the time needed for the nanobubble to lose enough gas via diffusion after the rate of change of surface area available to diffusion reaches stability, and is the same as the rate of change of surface area of the entire bubble. Thus, at the time equal to the summation of shrinkage times and the diffusion time t_d, the bubble can theoretically exist indefinitely. The value t_d can be found by the expression,

$$t_d \approx \frac{\delta^2}{2D} \qquad (25)$$

where D is the diffusion coefficient of the gas within the nanobubble.

However, this would require the outward diffusion to eventually reach zero, as the diffusion of the gas is completely blocked by the ions adsorbed on the surface at the saturation level. But, since the gas diffusion is never truly halted completely, it is evident that in the window

of time where the two rates of elimination and adsorption of hydroxide are unequal, diffusion occurs to a sufficient extent that the bubble shrinks, and establishing a new set of equilibrium conditions which are not met until the next set of equilibrium conditions, and this occurs until the nanobubble shrinks completely and disperses into the solution.

However, simulating the equations for velocity and from those, for the diffusion length presents us with a graph as shown below, for an assumed diameter of one micron.
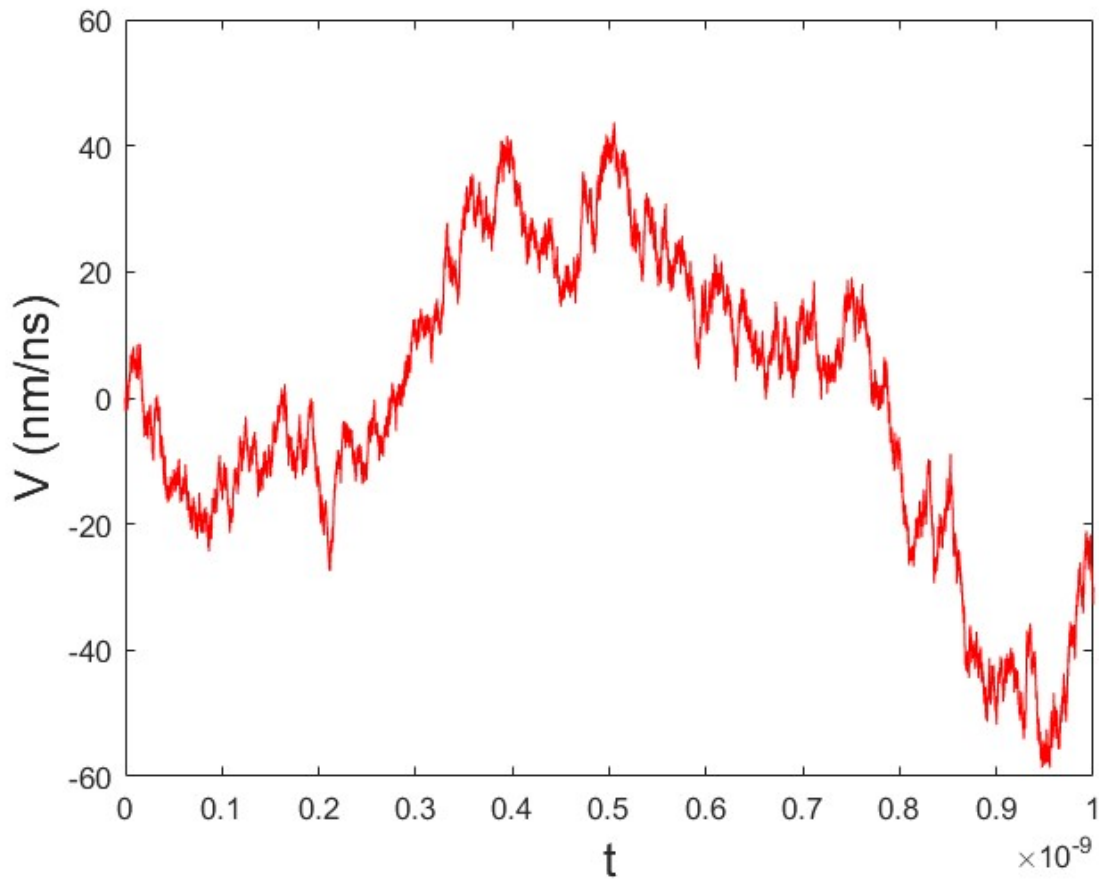
Figure 2: Plot of variation in velocity versus time due to Brownian motion.
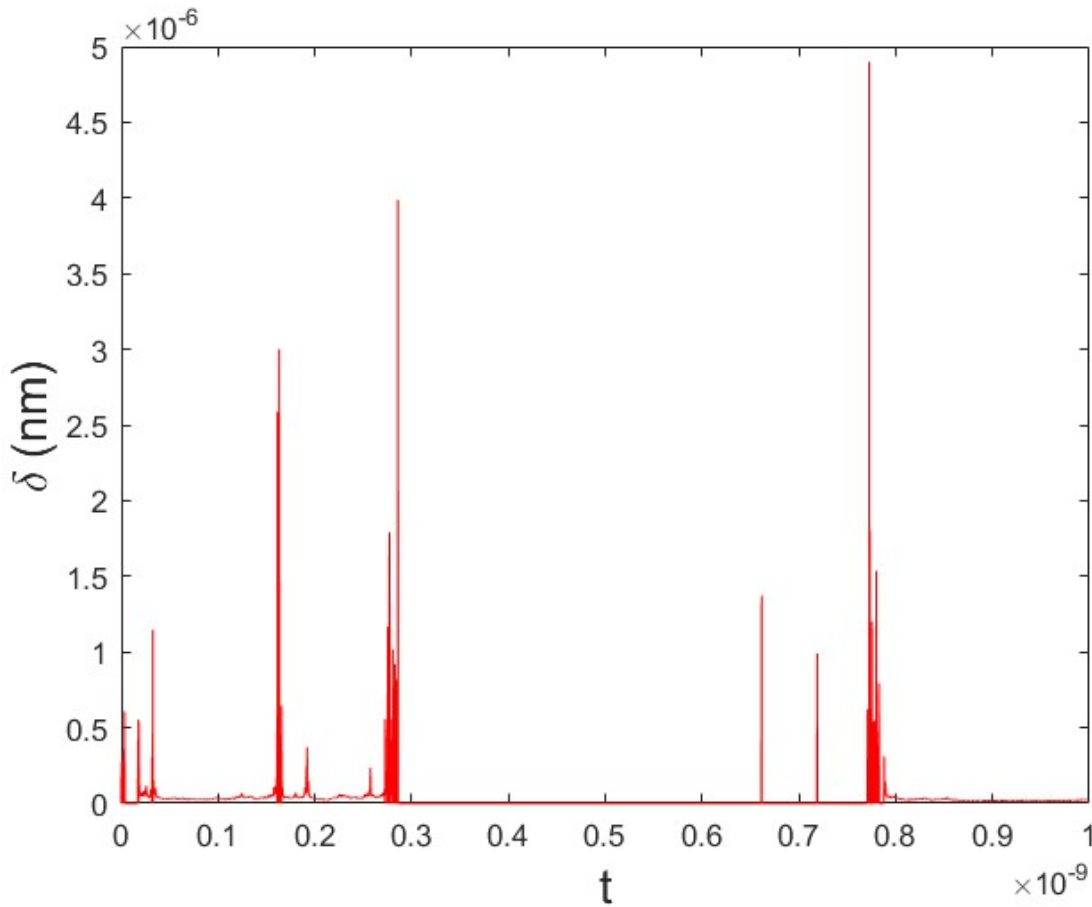
Figure 3: Plot of diffusion layer thickness to variation in Brownian motion velocity versus time.

It is clear from the data presented that, while the diffusion layer is, most of the time, near zero, it is, at brief instants, high enough that the entire volume of water surrounding the nanobubble will increase and decrease sufficiently to increase or decrease the diffusion rate by changing the thickness of the diffusion layer, and, by extension, the time of diffusion and the hence the time required for the bubble to reach stability. It is possible then, that a sufficient occurrence of these peaks could significantly change the lifetime of a nanobubble.

CHAPTER 5

5.1 Calculation of the Ionic Repulsion Force

In the derivation of the force balance presented in section 3.2, the formula takes into account the contribution of the repulsion between hydroxide ions adsorbed to the surface of the nanobubble. This section estimates the number of the ions adsorbed to the surface of the nanobubble, and uses the terms associated wit their arrangement to calculate this contribution and to examine the possibility that they can, indeed help to balance the inward and outward pressures exerted on the nanobubble surface and thus provide an explanation for their stability. Both possibilities of stationary and nanobubbles in motion are assumed and calculated to provide estimates for the repulsive force, and are substituted along with representative values in the derived equation for the force balance, and the result is presented.

5.2 Surface Charge and the Number of Adsorbed Ions

5.2.1 Stationary Bulk Nanobubble

The surface charge density can be calculated by the equation from the Debye-Hückel theory of electrical double layers,

$$\sigma = \frac{\epsilon \zeta}{\lambda_d} \qquad (26)$$

$$\lambda_d = \text{Debye length} = \sqrt{\frac{\epsilon k_B T}{2 \times 10^3 N_A e^2 I}} \text{ m} \qquad (27)$$

and ζ is the zeta potential, I is the molarity of the stabilising ions, i.e. the hydroxide ions which is 10^{-7} M at pH 7, T is temperature, k_B is Boltzmann's constant, N_A is Avogadro's number, e is electronic charge and ϵ is the absolute permittivity of the fluid, assumed to be pure water at 25°C. Considering the data reported by Ushikubo et al., we can take the zeta potential to be -35 mV for a bubble in ultrapure water at 25°C at pH 7, which allows us to use the value of the relative permittivity to be 78.304 as reported by Malmberg & Maryott [21], as well as to assume the concentration of hydroxide ions to be 10^{-7} M, and the Debye length from equation (14) is calculated to be λ_d = 960.4 nm, using the equation given by Russel and co-authors. Substituting it in the equation gives us an estimate for charge density σ = 2.524 × 10^{-23} C/nm². Using this value, dividing by unit charge to obtain the number of ions per area M,

$$M = \frac{2.524 \times 10^{-23}}{1.602 \times 10^{-19}} = 1.575 \times 10^{-4} \text{ ions/nm}^2 \qquad (28)$$

Considering the typical sizes of bulk nanobubbles reported, we can assume a representative diameter of 200 nm, which gives the number of ions to be approximately 20.

5.2.2 Bulk Nanobubble in Motion

However, the stationary nanobubble is an ideal case, and in actual situations the bulk nanobubble is usually in motion due to Brownian motion, which also prevents it from rising to the surface. Thus, it can be established that the bulk solvent for a bulk nanobubble in motion, only consists of the boundary layer that moves with the nanobubble as it moves through the solvent. It also must supply the ions needed to stabilise it, and must contain the ions that are adsorbed. We may use the Blasius solution of the Prandtl equation, since, by comparing the size of the nanobubble to the size of the water laminae we may approximate the relative curvature to be negligible, as well as the flow being laminar due to the fluid itself being static, and hence the flat plate approximation may apply. Thus, the approximate thickness of the boundary layer δ is obtained with equation (16) as before in section 4.4.

From Figures 2 and 3 for the same assumed conditions, we obtain a boundary layer thickness of about 60 microns. The exact volume of water available to interact with the nanobubble is, therefore about 9×10^{-19} litres. This, at pH 7, contains even less than one hydroxide ion, assuming uniform distribution of ions before the nanobubble is formed. Thus, drawing on the number of ions derived previously, even adding one ion to this volume significantly decreases the Debye length of the hydroxyl ions within the boundary layer. This in turn opens the possibility of pH being as high as 15 within the boundary layer, and the possibility of the number of ions being adsorbed being far larger. At pH 15, using the same equations as before, we obtain the Debye length to be 0.01 nm, with a corresponding surface charge of 2426 C, and the corresponding number of ions adsorbed to the surface being about 1.51×10^{22}. This, however, exceeds the number of hydroxyl ions that there is room for on the

surface, which is only about 1×10^6. This allows us to consider that the nanobubble surface might, in fact, be fully saturated, which, gives the Debye length a value of 0.2 nm, a corresponding surface charge of 1.21×10^{-18} C, and a pOH of 0.26, corresponding to a pH of 13.74.

5.3 Arrangement and Effects of Adsorbed Ions

5.3.1 Stationary Bulk Nanobubble

The inter-ionic distance, x, can also be found using equation (10), by substituting the same values used earlier for radius and the number of ions. This gives a value for x to be about 85 nm. Comparing with the Debye length of the hydroxyl ions at pH 7, which is given by equation (14), it is shown to be well within the range of electrostatic effects of the hydroxyl ions in solution. This also implies that any movement of the ion which would disturb it from its equilibrium position, such as the diffusion of gas out of the bubble, will have a high activation energy, thus reducing the rate of diffusion and providing an explanation for the long lifetimes of bulk nanobubbles.

5.3.2 Bulk Nanobubble in Motion

The inter-ionic distance for the completely saturated nanobubble is assumed to be zero, with ions being in direct contact with each other. While this is an extreme case, it remains possible. In this case, then, the ions would completely block the diffusion of the gas within the bubble to the bulk fluid by simple steric repulsion, giving the nanobubble a very long lifetime. However, since we do have a limit to the lifetime, it is clear that this extreme case does not exist, but it is likely that the reality approaches it, and that the pH of the boundary layer surrounding the nanobubble is significantly higher than the bulk solvent outside it.

5.4 Calculation of the Balanced Forces

Calculating the forces generated by ionic force and surface tension, using equation (12) and for the first case of a stationary nanobubble results in a value of the ionic force, for a nanobubble of diameter 200 nm and with 20 ions on its surface to be approximately 4×10^{-16} N, corresponding to a pressure of 3×10^{-3} Pa, and for surface tension, the calculated value is 4.5×10^{-8} N, corresponding to a pressure of 3.6×10^{5} Pa. For external pressure, assuming a water head height of 1m, the value is about 1×10^{5} Pa. Substituting these values in equation (3), an internal pressure of 5.6×10^{5} Pa is obtained. At 25°C, the number of moles of gas contained within the nanobubble determined from equation (5), n, to be 9.5×10^{-19} moles, or approximately 573,000 molecules.

However, for the case of a nanobubble in motion, with a diameter of 200 nm and the number of hydroxide ions adsorbed being 1×10^{6}, with the external conditions and surface tension being the same, the repulsive force is 2.5×10^{-10} N, corresponding to 2×10^{3} Pa. This gives a value for the internal pressure to be the same, about 9.4×10^{-19} moles, or approximately 569,000 molecules. Both of these numbers represent reasonable values for the number of moles of gas contained within the nanobubble.

In a second possible case, the force acting to shrink the nanobubble may be considered to be equal and opposite to the force of repulsion between hydroxyl ions that are adsorbed to the surface. In this case, considering the same zeta potential and radius as the previous calculations, the equations yield a value of approximately 2.1×10^{9} ions which is clearly not possible, with a Debye length of 8.5×10^{-15} m, which also gives an inter-ionic distance of

8.1×10^{-12} m. Since this distance is even smaller than the diameter of a hydroxyl ion, it is apparent that such a case cannot exist. Furthermore, the maximum number of ions that can be accommodated is approximately 1×10^{6}, whose force of repulsion is 2.6×10^{-10} N, which is not comparable to the force due to surface tension. Thus, it is concluded that hydroxyl ions adsorbed to the surface do not assist significantly in balancing the internal and external pressures of the nanobubble.

CHAPTER 6

6.1 Diffusion and the Adsorbed Ions

As stated in section 4.1, the other contributing factor to the change in the rate of diffusion is the effect of the hydroxide ions adsorbed to the surface. The mechanism of their actual inhibition would, conceivably be due to the steric hindrance imposed by them for an oxygen molecule attempting to leave the nanobubble. However, the spacing between the ions calculated in section 3.3.2 is far too high for any significant barrier to the diffusion. However, oxygen in gaseous state, that is to say, the oxygen molecule, is highly electronegative, and may offer significant repulsion to the hydroxide ions, as may other electronegative gases such as nitrogen. This would mean that the repulsive forces would, in theory require the ions adsorbed to the surface to change the spacing between them in order to permit the gas molecule to diffuse through an area free of the repulsion that force it to stay inside the nanobubble.

This also implies that any movement of the ion which would disturb it from its equilibrium position, such as the diffusion of gas out of the bubble, will have a high activation energy, thus reducing the rate of diffusion and providing an explanation for the long lifetimes of bulk nanobubbles. This possibility is analysed in this chapter, and can apply to oxygen, nitrogen and air, as it is a mixture of the two.

6.2 Kinetic Energy of the Gas and Diffusion

Takahashi et al. [14] report the zeta potential of microbubbles to be constant and independent of size, which, since the surface charge density is directly proportional to the zeta potential, implies that surface charge density is also constant. This indicates that the microbubble, as it shrinks, releases adsorbed ions from its surface in order to maintain the same surface charge density. We can assume that the shrinkage is thus opposed by the tendency of hydroxide ions to be de-adsorbed, since hydroxide ions appear to be in a lower energetic state when adsorbed to the surface of the nanobubble, than in solvation, which appears to be at a higher energy state. They would, therefore be forced to go into solution if the nanobubble cannot accommodate them on its surface due to shrinkage. However, for the nanobubble to shrink, the gas molecules contained within must escape, and to do so they must have sufficient momentum to provide the energy needed for the hydroxide ions adsorbed on the surface to be de-absorbed. Thus, the gas molecules require sufficient kinetic energy, which, when transmitted to the ions, must permit them to be de-adsorbed. We can also characterise this with a change in the force of repulsion between ions adsorbed on the surface and a change in the inter-ionic distance. We can then derive an expression for the minimum velocity needed by an oxygen molecule to escape the nanobubble, as,

$$\Delta E_{ions} = K.E._{gas\ molecule} \tag{29}$$

Assuming one hydroxide ion is forced into the solvated state from the adsorbed state,

$$\Delta E_{ions} = \Delta F_i.\Delta x = \left(\frac{(N-(N-1)\sqrt{3}k_e\sigma q)}{2}\right) \cdot \left[\sqrt{\frac{k_e\ q^2}{\frac{(N-(N-1)\sqrt{3}k_e\sigma q)}{2}}}\right] = \left[\sqrt{\frac{\sqrt{3}k_e\sigma q}{2}}\right] \tag{30}$$

Equating this to the kinetic energy of a molecule,

$$\left[\sqrt{\frac{\sqrt{3}k_e\sigma q}{2}}\right] = \frac{1}{2}mv^2 \qquad (31)$$

$$v = \sqrt{\frac{m}{2}\sqrt{\frac{\sqrt{3}k_e\sigma q}{2}}} \qquad (32)$$

where m is the mass of the gas molecule, and v is the minimum velocity it must have to escape the nanobubble. Since the velocity is inversely proportional to the square root of the radius, it increases as radius decreases, which provides a rationale for the lower diffusion rates of gas out of nanobubbles as compared to microbubbles. The velocity of the gas molecule must come from the Brownian motion of the molecules within the nanobubble, in the absence of any other driving forces, and may be counted as the root mean square velocity of a gas molecule as derived from kinetic gas theory.

However, the energy of the ions that the kinetic energy of the gas molecule needs to overcome, would, in effect, be the same as that which is used to inhibit the diffusion in the first place. Given the lack of any other factors, it is reasonable to assume the electrostatic repulsion between the hydroxide ions and the oxygen molecules to be the cause.

6.3 Inhibition of Diffusion

The hydroxide ions, then, clearly have a role in inhibiting diffusion of the gas molecules contained within the nanobubble into the bulk fluid. The mechanism for this inhibition is assumed to be by means of ion-lone pair repulsion, between the hydroxide ions adsorbed to the surface and the lone pairs of the oxygen atoms within the nanobubble. The surface of the bubbles, as shown earlier, is proposed to contain adsorbed hydroxide ions arranged in rhomboid unit cells, and by vector addition it is clear that the least repulsion to oxygen molecule to diffuse through the hydroxide ions would be at the centre of each rhombus, which would be limited to a greatly reduced area for the diffusion to occur through. This restriction would significantly increase the time needed for the gas to diffuse outward, causing the bubble to shrink at a much lower rate. Thus, the electrostatic repulsion would, in theory, be the weakest at the centre of each rhombus, and would presumably permit the number of oxygen molecules that can fit through it, as well as who have the requisite kinetic energy, to diffuse outward.

However, the number of the ions adsorbed to the surface causes difference to the limitation of outward diffusion. If, as in the second case, hydroxide ions are assumed to completely saturate the surface, then the diffusion is inhibited by the steric repulsion or steric hindrance of the hydroxide ions on the surface. This in turn will reduce the diffusion to nearly negligible levels, giving the nanobubbles highly increase lifetimes. While both the cases of stationary and moving nanobubbles represent two opposite sides of the spectrum of possible cases, it is clear that the trend of increasing number of adsorbed ions correlates to a decrease in the outward diffusion of gas and thus increased lifetimes of bulk nanobubbles.

6.4 Analysis of Ion-Gas Repulsion

The repulsion of the ions and the gas molecules is, essentially, a case of repulsion in aqueous solution, however, within the nanobubble, the case of the purely aqueous solution must be replaced with the case that the gas itself is a second medium with an interface. Thus, the solvent within the nanobubble becomes the oxygen gas and the ions are at the interface of the second medium. If the Gouy-Chapman theory of double layers is used, then the Debye length for the oxygen medium will approach infinity, and the effect of ionic repulsion extends throughout the nanobubble, allowing the hydroxide ions to repel oxygen molecules away from the interface and keeping them within the nanobubble and enabling them to balance the external pressure. The strength of the repulsive force would not be of the same level as the repulsion between, for example, two hydroxide ions, since the oxygen molecule is not charged, but the oxygen molecule also has two lone pairs in the valence shells of its constituent atoms, which can be repelled albeit much more weakly than an ion. If this conjecture is true, however, it will remain a valid mechanism for the inhibition of outward diffusion of electronegative gases from their respective nanobubbles.

This hypothesis is supported by the work of Meegoda and co-workers [23], who report increasing size and zeta potential with increasing electronegativity of the gas contained within the nanobubble. They report the largest size and the highest zeta potential for nanobubbles composed of ozone, followed by oxygen, followed by air and lastly of nitrogen. Their electronegativity is directly related to the number of lone pairs of electrons they possess. Thus, it is reasonable to suppose that the nature of the bond formed is a stronger version of the standard hydrogen bond between water molecules, due to the dipole moment

of the hydroxide ion. At the same time, however, the gas within the nanobubble also is repelled by the oxygen atom, the mechanism of which is by means of ion-lone pair repulsion, which would force the gas molecules to stay within the nanobubble, and hence severely limiting diffusion of the gas into the solvent.

However, as recently reported by Ushikubo [11], nanobubbles of inert gases do possess similar lifetimes and are formed from helium, neon, and argon, and since the only intermolecular forces of note they experience are van der Waal's forces of attraction, Lifshitz forces and dipole-dipole interactions, it can be assumed that these are also strong enough, and the gases sufficiently inert, for the same mechanism as well as the steric hindrance of the hydroxide ions to apply to the same case.

6.4.1 Analysis using the DLVO Theory

The DLVO theory is traditionally used to analyze the forces of attraction and repulsion between particles in colloidal suspension, but it can alternatively be applied, using a few appropriate assumptions, to also approximate the repulsion between hydroxide ions and oxygen molecules. The assumptions that I would like to present are:

1. We can think of the hydroxide ions and oxygen molecules as a system of molecules that are dissolved in free space, and that the 'solvent', thus, being free space does not interfere with the interactions between one hydroxide ion and one oxygen molecule.
2. The size of a hydroxide ion and an oxygen molecule is approximately the same, their actual sizes being 0.11 nm and 0.15 nm in radius, thus we can approximate them to be the median between them, 0.13 nm in radius.

3. The equivalent charge on oxygen molecule is some fraction of one electronic charge, and this fraction can be represented henceforth as f, with a value between 0 and 1, thus we can assign a charge to the oxygen molecules as fe, and a valency of $-f$.

That oxygen molecules are not polar in nature is confirmed, as the atoms have the same electronegativity. However, Gustafsson and Andersson [25] report the formation of induced dipoles in oxygen and nitrogen molecules adsorbed on platinum surfaces. Thus, it is conceivable that such a dipole may be formed by induction from the hydroxide ions adsorbed to the surface of the nanobubble, in any molecule that comes within sufficient distance (one Debye length) of the hydroxide molecule. Thus, it is then possible that a fractional effective charge, which we can use to quantify the electrostatic repulsion, can indeed exist and be responsible for the inhibition of diffusion.

The standard formula for the electrostatic force given by the DLVO theory in the form of a screened-Coulomb or Yukawa potential, is,

$$\beta U(r) = Z^2 \lambda_B \left(\frac{e^{\kappa a}}{1+\kappa a} \right) \frac{e^{-\kappa r}}{r} \tag{33}$$

where $\beta U(r)$ is the Yukawa potential, Z is the charge on the two particles, r is the centre-to-centre distance between them, κ is the inverse of the Debye length λ_D, λ_B is the Bjerrum length, and a is the radius of the ions. In the case defined above, a can be taken as the agreed upon value before, being 0.13 nm, and r being twice that, equal to 0.26 nm. Z, the charge will be the multiple of the two charges. Since the hydroxide ion has one electronic charge, and the oxygen molecule is expected to have f times that charge, Z^2 will therefore become fe^2. The Bjerrum length is found by the formula,

$$\lambda_B = \frac{e^2}{4\pi\epsilon_0 k_B T} \tag{34}$$

which gives us a value of 5.608×10^{-8} m. The Debye length, however, is a more complex

phenomenon. Essentially, we need to consider the effects of the hydroxide ions and the

oxygen molecules together as one single type of particle solvated in free space, which may

be approximated by a number average charge distributions and the net number of particles

in the nanobubble, of both gas and hydroxide ions. The number of particles, according to

previous sections, is about 1,573,000, and the number average of the charge, represented by

θ, is given by,

$$\theta = \frac{e(1,000,000) + fe(573,000)}{1,573,000} = e(1 + f) \tag{35}$$

The exact formula for the Debye length is,

$$\lambda_D = \left(\frac{\varepsilon k_B T}{\sum_{j=1}^{N} n_j^0 \theta_j^2}\right)^{1/2} \tag{36}$$

The value obtained by substituting equation 35 and the values from above, with the

permittivity of free space and 298 K for temperature, we get a Debye length of

$3.8 \times 10^{-10}/(1+f)^{1/2}$. Substituting it in the equation (33), we get a value for the potential to

be

$$\beta U(r) = (1 + f)(5.535 \times 10^{-36})\left(\frac{e^{\left(-4.94(1+f)^{1/2}\right)}}{1 + \left(4.94(1+f)^{1/2}\right)}\right) \tag{37}$$

Thus, the approximate potential we obtain is not zero, as would be the case if there was no

repulsion, even if f is zero. However, since f cannot be zero since oxygen does not form an

non-polar molecule, we know a significant repulsion can, indeed, exist between hydroxide

ions and oxygen molecules to inhibit the outward diffusion of the molecules.

CHAPTER 7

7.1 Results

7.1.1 pH Dependence

The pH dependence of bulk nanobubble formation can also be analysed using this equation. Considering the formation of a 1 μm microbubble which eventually shrinks into a nanobubble, the number of ions available to it for stabilisation from the water it displaces upon formation, at pH 7, is approximately 33 ions, which if all the ions were adsorbed, does not agree with the zeta potentials reported by Takahashi et. al. for microbubbles of comparable size [8], which by equation (8) is given to be approximately 495 ions. It follows that the ions which are adsorbed diffuse toward the nanobubble surface from the surrounding bulk fluid, which can explain the apparent generation of free radicals observed by Takahashi et. al. [23], since there is now a minuscule concentration difference present to drive the diffusion. The availability of hydroxide ions also depends on the pH, and at pH 7 it is thus possible for stable nanobubbles to form as is reported by Ushikubo [11], as well providing a mathematical treatment for their stabilization and the calculation of their surface charge. At lower pH, in the absence of other ions, the concentration of stabilized ions would be lower due to the lower availability of hydroxide ions and the increased time needed for them to diffuse to the surface of the nanobubble, allowing it more time to shrink.

7.1.2 External Pressure Dependence

The dependence of the size of the bulk nanobubble on external pressure is given by equation (12). Of the external pressure, the proportion of the atmospheric pressure to the total value of the actual pressure, the rest being the pressure exerted by the fluid. However, the major component to the force contributing to the shrinkage of the nanobubble is the surface tension, which also increase with the size of the nanobubble.

Thus, for higher external pressures and given that a limited amount of gas is dissolved in the fluid, the equation gives a trend of increasing nanobubble size with increasing external pressure. However, due to the limited amount of gas available, it is expected that the number of nanobubbles formed, i.e. concentration will decrease, while still giving higher particle size. This is confirmed by Tuziuti and co-workers through their observations of air nanobubbles in water [24].

7.1.3 Temperature Dependence

The temperature term appears only in the term that describes the internal pressure, causing a linear increase with temperature, not taking into account the increase in molecular motion due to heat, as well the increased energy of the surface ions. Thus, it also shows that the internal pressure will increase with the increase in temperature. This will, in turn, cause a reduction in the radius if all other terms are kept the same.

Thus, we can say that given a limited amount of gas dissolved in the solvent, an increase in temperature will give smaller nanobubbles, but will also cause an increase in concentration of the nanobubbles in the solvent. It is also possible that zeta potentials may decrease, as thermally agitated hydroxide ions may be more susceptible to de-adsorption and may return to solution more easily.

Conversely, as lower temperatures, larger bubbles may form, especially by the method of collapsing microbubbles, and larger numbers of hydroxide ions may be adsorbed on the surface of the nanobubble, giving longer lifetimes.

CHAPTER 8

8.1 Potential Future Applications

Bulk nanobubbles are, in essence, minuscule voids of gas carried in a fluid medium, with the ability to carry objects of the appropriate nature, that is, positively charged for a length of time that is significant, if the nanobubble is left alone, yet is also controllable, since the bubbles can be made to collapse with ultrasonic vibration, or magnetic fields. The applications, then, seem to be limited only by how we can manipulate and design systems that make use of these properties for new technology in several fields. As mentioned before, thus far technology has made use of the uncontrolled collapse and generation of bulk nanobubbles, in the fields of hydroponics, pisciculture, shrimp breeding, and algal growth, while the property of emission of hydroxide ions during collapse has been applied to wastewater treatment. Here and there, there are indications of greater possibilities, as evidenced by research into their ability to remove microbial films from metals, to remove calcium carbonate and ferrous deposits from corroded metal, the use of hydrogen nanobubbles in gasoline to improve fuel efficiency, and the potential application for to serve as nucleation sites for crystals of dissolved salts. The following sections elaborate on further applications which are possible in the near future.

8.2 Proton Exchange Membrane Fuel Cells

Proton exchange membrane fuel cells, (PEMFCs) are finding wide application in several fields due to the ease of their deployment, the low start-up times, and the convenience of their size and operating temperatures (9). However, significant limitations exist for their wider application, which can broadly be classed under the headings of catalysis, ohmic losses, activation losses, and mass transfer losses.

The first of these is due to the rate of catalysis of the splitting of hydrogen, which cannot be pushed beyond a certain limit due to the constraints of temperature. But the larger issue is the cost of the catalyst itself, which is a combination of platinum nanoparticles and graphite powder, which provides the electrical conductivity. The inclusion of platinum presents a significant cost disadvantage, and while efforts are ongoing to reduce or replace platinum as a catalyst, these are still experimental and much research is ongoing in this field.

The second limitation is due to ohmic losses, which accumulate due the proton exchange membranes, also termed the electrolyte, and can only be reduced by reducing the thickness of the membrane. Current popularly used membranes are usually made of Nafion, a sulphonate-grafted derivative of polytetrafluoroethylene (PTFE) marketed by DuPont, but experimental membranes include the use of graphene, aromatic polymers, and other similar materials which possess a high selective conductivity toward protons [ref]. However, beyond a certain thickness the membranes are unable to mechanically support themselves, and often mechanical failure of the membrane will cause a break in operations.

The third limitation is due to the start-up conditions of the fuel cell, and are a matter of the mechanics of operation of the fuel cell itself. The last limitation is due to the transport of hydrogen and oxygen to the triple phase boundaries around the catalyst and the transport of water away from them, and is a significant concern for the operation and efficiency of PEMFCs.

However, the current PEMFCs depend on gaseous hydrogen and oxygen, which are released from a compressed source and derived from air respectively. This necessitates a mechanically strong membrane and construction to resist the operating pressures. However, the inclusion of the gas as a nanobubble dissolved in water presents new possibilities, used in combination with microfluidic technology. It becomes possible to also replace both membranes and catalysts with materials that have been hitherto discarded fro being too mechanically weak, such as graphene, and the possibility of using graphene as a combined catalyst and proton exchange membrane, as nanobubbles of hydrogen and air, dissolved in water, to act as the reservoirs for the fuel and oxidant.

Such as system would operate on the basis that nanobubbles are negatively charged, and would hence be attracted to the graphene through which current would be passed in order to activate the process. Air and hydrogen nanobubbles would be separated by the graphene membrane, and be adsorbed to opposite sides of it. The graphene membrane would also have a potential difference applied across it in the plane of the graphene layer. This would, in turn, permit the hydrogen to be catalyzed to protons [ref], and hence be conducted across the graphene [ref], allowing it react with the oxygen to form more water, which would be carried

away with the flow. Microfluidic bipolar plates would enable the construction of such a device, and such fuel cells could become the future source of energy for several applications.

The advantages of such a system would be numerous. Firstly, graphene is far cheaper than platinum, and can be used as a catalyst of almost comparable quality, in addition to also being the conductor for the removal of electrons released during catalysis. Secondly, the thickness of a graphene sheet is in the range of nanometers, which would mean that ohmic losses would, quite possibly, be nearly eliminated. Additionally, due to the flow of water as a solvent, the losses due to the mass transport of water away from the triple phase boundary, and that due to transport of hydrogen and oxygen to the triple phase boundary, would also be significantly reduced. The last, but not the least advantage would be the reduction in the size of one fuel cell. The voltage generated by fuel cells is independent of the size they are, which would mean that a much larger number of fuel cells can fit in the same area as currently applied fuel cells, which will provide a much larger voltage.

8.3 Polymeric Nanofoams

Polymeric foams have been a staple of several products since their inception, and pore size is one of the key properties of the foam that determines its performance. In general, the larger the pore size, and more the pore count, the lighter the foam is. However, both can come at the cost of reduced wall thickness of the pores, which makes the whole foam less able to deform elastically and more susceptible to tearing and heat damage, while substantially reducing fatigue resistance and creep resistance. In general, therefore, the standard practice is to achieve a balance between pore size and pore count, measured in pores per volume, so as to achieve the desired properties.

However, the voids rarely go below the size of one micron, and this in turn places a limit on the number of pores per volume, thus limiting the number of pores it is possible to introduce, as well as the amount of gas that can be introduced into the foam system. While there are several methods of foam manufacturing, including in-situ foam molding, and pre-mixed foam molding, none of these offer pore sizes lower than a few microns reliably and controllably. Furthermore, many of the polymers used in the construction of these foams can either be dispersed or dissolved into water, such as polyamides, polystyrene, polyesters, and polyurethanes. This offers a unique opportunity to introduce nanobubbles into the system, by first dispersing the gas into solution by means of a microbubble generator, and then dispersing the polymer, either in dilute solution form or as a monomer, and then either coagulating the dispersion, or polymerizing it, or crosslinking the chains in solution to create a foam with pore sizes in the nanometer range. At standard pore counts, this would offer a very high wall thickness, which necessitates a large increase in the concentration of

nanobubbles which should be introduced to return wall thickness to the same levels as a microporous foam. The pores can then be opened, if so desired, by a microneedle array, or by other methods such as guided bursts of ultrasound, creating such structures as channels only nanometers in width through the foam, and presenting new possibilities for water filtration and purification, as well as for testing and for further application in water quality testing and other similar applications.

As of now, there are several applications for such open-celled foams, such as the production of nanopure water, which are expensive due to the filtration equipment needed. Thus, open-celled polymeric foams have direct application to these areas, where as closed-celled foams are potentially lighter and stronger, as well as tougher than other foams with larger pores and lower pore counts. Thus, it is reasonable to suggest that nanobubble technology will find widespread use in this particular application, especially when the cost factor is taken into account.

CHAPTER 9

9.1 Conclusions

The present work has shown that the repulsive force of hydroxyl ions adsorbed to the surface of the nanobubble may be comparable to the external pressure and surface tension, and that a relatively large internal pressure is required to balance them. However, it appears that the required internal pressure is possible due to the inhibition of outward diffusion of the gas inside the nanobubble by a sufficiently high concentration of hydroxyl ions at the bubble surface. This concentration of ions is made possible by the shrinkage of larger microbubbles that start with a concentration of ions at their surface that is dictated by the pH of the solution.

The effects of Brownian motion serve to increase the concentration of ions at the nanobubble surface by changing the size of the boundary layer thickness of the water around the nanobubble, and thus increase the effects of the hydroxide ions adsorbed to the nanobubble. These lie mainly in the ability of the ions to produce a force of repulsion strong enough to possibly balance the surface tension, and, due to the high concentration, to inhibit the outward diffusion of gases from the nanobubble. This contributes to their stability and provides an explanation for their long lifetimes.

The present model indicates that, as the concentration of ions at the nanobubble surface increases as the microbubble shrinks, the ions will be able to inhibit outward gas diffusion as the bubble diameter reaches a range commonly observed for stable nanobubbles.

9.2 Summary

The theory of the stability of bulk nanobubbles presented here is, in brief, an explanation for the stability which uses the hydroxide ions adsorbed to the surface of a nanobubble as an agent for a force to balance the large surface tension experienced by the nanobubble surface. It is concluded that while the surface tension and external pressure that seek to shrink the bubble are indeed very strong forces, they can be balanced by the repulsion between adjacent ions adsorbed to the surface of the ions, as well as the internal pressure of the gas contained within the nanobubble.

The pressure of the gas within the nanobubble however, is only made possible by the inhibition of the outward diffusion by the same ions adsorbed to the surface. Thus, the adsorbed ions play two important roles. Firstly, they may be able to repel surface tension when the separation between them, or the inter-ionic distance is extremely low. This would balance the surface tension and negate the pressure gradient the gas within the nanobubble experiences, reducing the outward diffusion. Secondly, they also physically inhibit the outward diffusion of the gas by reducing the surface area that is left unoccupied by them for the gas to diffuse out through. They may also be repelling the gas, if its molecules are electronegative enough, to force them to stay within the nanobubble.

The above listed effects of the adsorption of hydroxide ions onto the nanobubble surface culminate into observable effects on the size of the nanobubble in response to changes in variables of state, such as pH, temperature, and external pressure. The effects, respectively are: for a decrease in pH, we obtain smaller sizes and larger concentrations of nanobubbles, and vice versa, for an increase in temperature, we obtain smaller sizes and smaller

concentrations of nanobubbles and vice versa, and for increasing external pressure we obtain smaller sizes and larger concentration of nanobubbles. The lifetimes can also be estimated by the sizes of the nanobubbles, enabling the design of systems that respond to these changes and can be used in meaningful ways in systems such as proton-exchange membrane fuel cells, nanofoams, sewage treatment, et cetera.

REFERENCES

1. Ljunggren, S., Eriksson, J. C., (1997), The lifetime of a colloid-sized gas bubble in water and the cause of the hydrophobic attraction, *Colloids Surfaces A. Physicochem. Eng. Aspects,* (129-130), 151-155,.

2. Seddon, J. R. T., Lohse, D., Ducker, W. A., Craig, V. S. J., (2012), A Deliberation on Nanobubbles at Surfaces and in Bulk, *ChemPhysChem,* (13), 2179 – 2187.

3. Attard, P., Moody, M. P., Tyrrell, J. W. G., (2002) Nanobubbles: the big picture, *Physica A: Statistical Mechanics and its Applications,* (314)1, 696-705.

4. Attard, P., (2015), Thermodynamic Stability of Nanobubbles, arXiv.org.

5. Brenner, M. P., Lohse, D., (2008), Dynamic Equilibrium Mechanism for Surface Nanobubble Stabilization, *Phys. Rev. Lett.*, (101), 214505-1 – 4.

6. Weijs, J.H., Lohse, D., (2013), Why Surface Nanobubbles Live for Hours, *Phys. Rev. Lett.*, (110), 054501-1 – 054501-2.

7. Sverdrup, K., Kimmerle, S. J., Berg, P., (2017), Computational investigation of the stability and dissolution of nanobubbles, *Applied Mathematical Modelling,* (49), 199–219.

8. Takahashi, M., (2005), ζ Potential of Microbubbles in Aqueous Solutions: Electrical Properties of the Gas–Water Interface, *The Journal of Physical Chemistry B*, (109) 46, 21858-21864.

9. Zangi, R., Engberts. J. B. F. N., (2005), Physisorption of Hydroxyl Ions from Aqueous Solution to a Hydrophobic Surface, *J. Am. Chem. Soc.*, (127), 2272-2276.

10. Yasui, K., Tuziuti, T., and Kanematsu, W., (2018), Mysteries of bulk nanobubbles (ultrafine bubbles); stability and radical formation, *Ultrasonics – Sonochemistry*, (48), 259 – 266.

11. Ushikubo, F. Y., Enari, M., Furukawa, T., Nakagawa, R., Makino, Y., Kawagoe, Y., Oshita, S., (2010), Zeta-potential of Micro- and/or Nano-bubbles in Water Produced by Some Kinds of Gases, *IFAC Proceedings Volumes,* (43) 26, 283-288.

12. Jin, F., Li, J., Ye, X., Wu, C., (2007), Effects of pH and Ionic Strength on the Stability of Nanobubbles in Aqueous Solutions of α-Cyclodextrin, *The Journal of Physical Chemistry B*, (111)4, 11745-11749.

13. Ahmed, A. K. A., Sun, C., Hua, L., Zhang, Z., Zhang, Y., Marhaba, T., Zhang, W., (2018), Colloidal Properties of Air, Oxygen, and Nitrogen Nanobubbles in Water: Effects of Ionic Strength, Natural Organic Matters, and Surfactants, *Environmental Engineering Science*, (35)7.

14. Agarwal, A., Ng, W. J., Liu, Y., (2011), Principle and applications of microbubble and nanobubble technology for water treatment, *Chemosphere*, (84), 1175-1180.

15. Endo. A., Srithongouthai, S., Nashiki, H., Teshiba, I., Iwasaki, T., Hama, D., Tsutsumi H., (2008), DO-increasing effects of a microscopic bubble generating system in a fish farm, *Marine Pollution Bulletin*, (54), 78-85.

16. Srithongouthai, S., Endo, A., Inoue, A., Kinoshita, K., Yoshioka, M., Sato, A., Iwasaki, T., Teshiba, I., Nashiki, H., Hama, D., Tsutsumi, H., (2006), Control of dissolved oxygen levels of water in net pens for fish farming by a microscopic bubble generating system, *Fisheries Science*, (72), 485-493.

17. Oha, S. H., Han, J. G., Kim, J. M., (2015), Long-term stability of hydrogen nanobubble fuel, *Fuel*, (158), 399–404.

18. Cai, W. B., Yang, H. L., Zhang, J., Yin, J. K., Yang, Y. L., Yuan, L. J., … Duan, Y. Y. (2015). The Optimized Fabrication of Nanobubbles as Ultrasound Contrast Agents for Tumor Imaging, *Scientific reports*, 5, 13725.

19. Hirose, Y., Yasui, T., Taguchi, K., Fujii, Y., Niimi, K., Hamamoto, S., Okada, A., Kubota, Y., Kawai, N., Itoh, Y., Tozawa, K., Sasaki, S., Kohri, K., (2013), Oxygen nano-bubble water reduces calcium oxalate deposits and tubular cell injury in ethylene glycol-treated rat kidney, *Urolithiasis*, (41) 4, 279-294.

20. Abida, H. S., Laliab, B. S., Bertoncelloa, P., Hashaikehb, R., Cliffordc, B., Gethinc, D. T., Hilala, N., (2017), Electrically conductive spacers for self-cleaning membrane surfaces via periodic electrolysis, *Desalination*, (416), 16-23.

21. Malmberg, C. G., Maryott, A. A., (1956) Dielectric Constant of Water from 0 to 100° C, *Journal of Research of the National Bureau of Standards*, (56) 1.

22. Takahashi, M., Chiba, K., Li, P., (2007), Free-Radical Generation from Collapsing Microbubbles in the Absence of a Dynamic Stimulus, *The Journal of Physical Chemistry B*, (111), 1343-1347.

23. Meegoda, J. N., Hewage, S. A., Batagoda, J.H., (2018), Stability of Nanobubbles, *Environmental Engineering Science*, (35)11.

24. Tuziuti, T., Yasui K., Kanematsu, W., (2017), Influence of increase in static pressure on bulk nanobubbles, *Ultrasonics Sonochemistry*, (38), 347-350.

25. Gustafsson, K., Andersson, S., (2006), Dipole active vibrations and dipole moments of N2 and O2 physisorbed on a metal surface, *The Journal of Chemical Physics*, (125)4, 044717.

26. Matsuki, N., Ishikawa, T., Ichiba, S., Shiba, N., Ujike, Y., Yamaguchi, T., (2014), Oxygen supersaturated fluid using fine micro/nanobubbles, *International Journal of Nanomedicine*, (9), 4495–4505.

27. Kim, J. Y., Song, M. G., Kim, J. D., (2000), Zeta Potential of Nanobubbles Generated by Ultrasonication in Aqueous Alkyl Polyglycoside Solutions, *Journal of Colloid and Interface Science*, (223), 285–291.

28. Attard, P., (2013), Nanobubbles and the hydrophobic attraction, *Advances in Colloid and Interface Science*, (104), 75–91.

29. Attard, P., (2016), Pinning Down the Reasons for the Size, Shape, and Stability of Nanobubbles, *Langmuir*, (32) 43, 11138-11146.

30. Epstein, P. S., Plesset, M. S., (1950), On the Stability of Gas Bubbles in Liquid-Gas Solutions, *The Journal of Chemical Physics,* (18), 1505-1509.

31. Gurunga, A., Dahla, O., Jansson, K., (2016), The fundamental phenomena of nanobubbles and their behavior in wastewater treatment technologies, *Geosystem Engineering*, (19) 3, 133–142.

32. Jia, W., Ren, S., Hu, B., (2013), Effect of Water Chemistry on Zeta Potential of Air Bubbles, *International Journal of Electrochemical Science*, (8), 5828 – 5837.

33. Knüpfer, P., Ditscherlein, L., Peuker, U. A., (2017), Nanobubble enhanced agglomeration of hydrophobic powders, *Colloids Surfaces A. Physicochem. Eng. Aspects*, (530), 117-123.

34. Mazumder, M., Bhushan, B., (2011), Propensity and geometrical distribution of surface nanobubbles: effect of electrolyte, roughness, pH, and substrate bias, *Soft Matter*, (7), 9184.

35. Petsev, N. D., Shell, M. S., Leal, L. G., (2013), Dynamic equilibrium explanation for nanobubbles' unusual temperature and saturation dependence, *Physical Review E*, (88), 010402-1 – 5.

36. Zhu, J., An, H., Alheshibri, M., Liu, L., Terpstra, P. M. J., Liu, G., Craig, V. S. J., (2016), Cleaning with Bulk Nanobubbles, *Langmuir*, (32), pg. 11203–11211, 2016.

BIBLIOGRAPHY

1. Tsuge, H. (Eds.), (2015), *Micro- and Nanobubbles: Fundamentals and Applications*, Boca Raton, FL: CRC Press.

2. Russel, W.B., Saville, D.A., Schowalter, W. R., (1989) *Colloidal Dispersions*, New York, NY: Cambridge University Press.

3. Israelachvili, J., (2011), *Intramolecular and Surface Forces*, 3rd Ed., San Diego, CA: Academic Press.

4. Van Oss, C. J., (2008), *The Properties of Water and their Role in Colloidal and Biological Systems*, San Diego, CA: Academic Press.

5. James, A. P., Lord, M. P., (1992) *Macmillan's Chemical and Physical Data*, Basingstoke, UK: MacMillan Press.

6. Coffey, W. T., Kalmykov, Y. P., Waldron, J. T., (2004) *The Langevin Equation With Applications to Stochastic Problems in Physics, Chemistry and Electrical Engineering*, Hackensack, NJ: World Scientific Publishing Co.

7. Lemons, D. S., (2002), *An Introduction to Stochastic Processes in Physics Containing "On the Theory of Brownian Motion" by Paul Langevin, translated by Anthony Gythiel*, Baltimore, MD: Johns Hopkins University Press.

8. Cengel, Y., Cimbala, J., (2014), *Fluid Mechanics: Fundamentals and Applications*, New York, NY: McGraw-Hill Education.

9. O'Hare, R., Cha, S. W., Collela, W. G., Prinz, F. B., (2016), *Fuel Cell Fundamentals*, Hoboken, NJ: John Wiley & Sons.

APPENDIX A

MATLAB code for Figures 2 and 3

MATLAB Code for Figure 2

```matlab
randn('state',100)              % set the state of randn
T = 0.000000001; N = 100000; dt = T/N;
n = 1.3185*(10e-9);
M = 0.032;
gamma = 0.072;
tb = M*n/gamma;
m = n/M;
dW = zeros(1,N);                % preallocate arrays ...
W = zeros(1,N);                 % for efficiency

dW(1) = sqrt(dt)*randn;         % first approximation outside the
loop ...
W(1) = dW(1);                   % since W(0) = 0 is not allowed
for j = 2:N
   dW(j) = 1/m*exp(-(T-dt*j)/tb)*sqrt(dt)*randn;   % general
increment
   W(j) = W(j-1) + dW(j);
end

plot([0:dt:T],[0,W],'r-')       % plot W against t
xlabel('t','FontSize',16)
ylabel('V(nm/ns)','FontSize',16,'Rotation',90)
```

MATLAB code for Figure 3

```matlab
randn('state',100)               % set the state of randn
T = 0.000000001; N = 100000; dt = T/N;
n = 1.3185*(10e-9);
M = 0.032;
gamma = 0.072;
tb = M*n/gamma;
m = n/M;
dW = zeros(1,N);                 % preallocate arrays ...
W = zeros(1,N);                  % for efficiency

dW(1) = sqrt(dt)*randn;          % first approximation outside the
loop ...
W(1) = dW(1);                    % since W(0) = 0 is not allowed
for j = 2:N
   dW(j) = 1/m*exp(-(T-dt*j)/tb)*sqrt(dt)*randn;   % general
increment
   W(j) = W(j-1) + dW(j);
end

one_matrix = ones(1, 10^5);
temp = 0.00089*10e-9*2*3.1416*(10e-6);
temp = one_matrix.*temp;

del = 4.91*sqrt(temp./W);
k = del*-sqrt(-1);
plot([0:dt:T],[0,k],'r-')        % plot W against t
xlabel('t','FontSize',16)
ylabel('\delta (nm)','FontSize',16,'Rotation',90)
```